www.sciencemag.org/cgi/content/full/322/5899/265/DC1

Supporting Online Material for

Small Molecule–Induced Allosteric Activation of the *Vibrio cholerae* RTX Cysteine Protease Domain

Patrick J. Lupardus, Aimee Shen, Matthew Bogyo,* K. Christopher Garcia*

*To whom correspondence should be addressed. E-mail: mbogyo@stanford.edu (M.B.); kcgarcia@stanford.edu (K.C.G.)

Published 10 October 2008, *Science* **322**, 265 (2008)
DOI: 10.1126/science.1162403

This PDF file includes:

Supporting Online Material

Materials and Methods

Bacterial and eukaryotic cell growth conditions. Bacterial strains were grown at 37ºC in Luria-Bertrani (LB) broth. Antibiotics were used at 100 μg/mL carbenicillin for pET22b and pGP704-Sac28 vectors in *E. coli* and *V. cholerae* and 30 μg/mL kanamycin for pET29b vectors in *E. coli*. HFF cells were grown in DMEM supplemented with glutamine and 10% fetal bovine serum (FBS) and maintained at 37ºC in a 5% CO_2-air atmosphere.

Plasmid and strain construction. Primers used are listed in table S3. For construction of His_6-tagged full-length CPD, pET28a-CPDstop expression constructs were generated by PCR-amplifying DNA corresponding to RTX amino acids 3391-3650 from *Vibrio cholerae* N16961 genomic DNA using primers #001 and #002. A TAA stop codon was inserted after the codon coding for amino acid 3650 in the 3' primer. PCR fragments were cloned into the NdeI/XhoI sites of the pET28a expression vector (Novagen). Point mutations were introduced by PCR splicing by overlap extension (SOE) (*1*). To generate C-terminally His_6- and BirA-tagged cleaved CPD, the pET22b expression was modified to insert a sequence encoding the BirA biotinylation site (LHHILDAQKMVWNHR) upstream of the C-terminal His_6-tag encoded by pET22b. 5' phosphorylated primers (#041 and #042) encoding the biotinylation site were annealed together to generate a DNA fragment with overhangs compatible with the SalI/ XhoI sites of pET22b. This allowed construction of a pET22b-BirA vector and generation of pET22-cCPD-BirA expression constructs by ligating NdeI/SalI digested PCR-amplified DNA fragments corresponding to RTX amino acids 3442-3650. pET28a-CPD stop constructs (including mutant constructs) were used as template DNA.

To construct point mutations in *V. cholerae*, double homologous recombination using the *sacB*-lethality counterselection method was used (*2*). PCR SOE was used to amplify a 1.2 kB fragment with ~0.5 kB of homologous sequence flanking the point mutation. The flanking primers used for the SOE reaction were #35 and #36, while the internal primers were #21 and #22 (W192A), #23 and #24 (C140A), and #32 and #33 (R182Q/K183N). The *rtxA* deletion mutant was constructed by performing PCR SOE to generate an in-frame deletion fragment that removes amino acids 14-4557 of RTX. The flanking primers were #37 and #38, and the internal SOE primers were #39 and #40. PCR fragments were ligated into the sucrose-based counter selectable plasmid pGP704-Sac28 using the NcoI/XbaI sites (*3*). Allelic exchange plasmids were transformed into *E. coli* SM10λpir and mated into the recipient *V. cholerae* strain. Consistent with previous studies of *V. cholerae* RTX function, the *V. cholerae* N19691 strain referred to as wildtype contains an in-frame deletion in *hapA* to reduce heterologous proteolysis of RTX (*4-6*). Sucrose-based counter selection was done essentially as described (*6*), and mutations were confirmed by PCR and genomic DNA sequencing.

***In vitro* CPD cleavage assay.** Autocleavage of N-terminally His_6-tagged CPD variants (corresponding to RTX amino acids 3391-3650) was performed in 75 μL reaction volumes containing 1 μM CPD enzyme in cleavage assay buffer (60 mM NaCl, 20 mM Tris pH 7.5, 250 mM sucrose). Inositol hexakisphosphate ($InsP_6$, Calbiochem), inositol (1,3,4,5,6) pentakisphosphate (Ins(1,3,4,5,6)P_5, Calbiochem), or inositol (1,4,5,6) tetrakisphosphate (Ins(1,4,5,6)P_4, Sigma) were added to cleavage reactions at a 1:100 dilution to give the indicated concentrations. Guanosine 5′-[γ-thio]triphosphate (GTPγS, Sigma) was added at a 1:10 dilution. Cleavage reactions were incubated at 37ºC for 2 h, after which autocleavage was stopped by the

addition of SDS-PAGE loading buffer. Samples were boiled for 3 min at 95ºC and resolved by SDS-PAGE on 15% gels. Cleavage reactions were visualized by Coomassie staining and quantified using the program ImageJ (http://rsb.info.nih.gov/ij/). The amount of autocleaved protein relative to the total protein amount was plotted versus concentration of ligand. The AC_{50} (the concentration of ligand that produced half-maximal cleavage) was determined from these plots using the Michaelis-Menten function on KaleidaGraph.

Protein expression and purification. For purification of N-terminally His_6-tagged CPD variants used in enzyme assays, overnight cultures of the appropriate strain were diluted 1:500 in 500 mL 2YT media and grown shaking at 37ºC. When an OD_{600} of 0.6 was reached, IPTG was added to 350 µM, and cultures were grown for 4 hr at 30ºC. Cultures were pelleted, resuspended in 25 mL lysis buffer [500 mM NaCl, 50 mM Tris-HCl, pH 7.5, 15 mM imidazole, 10% glycerol] and flash frozen in liquid nitrogen. Lysates were thawed, then lysed by sonication and cleared by centrifugation at 15,000 x g for 30 minutes. His_6-tagged CPD (amino acids 3391-3650) was affinity purified by incubating the lysates in batch with 0.5 mL Ni-NTA Agarose beads (Qiagen) with shaking for 1 hr at 4ºC. The binding reaction was pelleted at 1,500 x g, the supernatant was set aside, and the pelleted Ni-NTA agarose beads were washed 3 x with lysis buffer. His_6-tagged CPD was eluted from the beads by the addition of 250 µL elution buffer [500 mM NaCl, 50 mM Tris-HCl, pH 7.5, 175 mM imidazole, 10% glycerol]. The affinity pull-down was repeated on the reserved supernatant to maximally recover His_6-tagged CPD proteins. Purified His_6-tagged CPD proteins were stored at -20ºC in elution buffer.

Wildtype and mutant cleaved CPD (amino acids 3442-3650) containing a C-terminal BirA biotinylation sequence (LHHILDAQKMVWNHR) and a His_6-tag were affinity purified as

described above. The purified samples were buffer exchanged into gel filtration buffer [250 mM NaCl, 10 mM Tris-HCl pH 7.5] and further purified by gel filtration chromatography using an S200 16/60 Sephacryl column (GE Healthcare). Protein fractions were pooled and concentrated in a low salt buffer [100 mM NaCl, 10 mM Tris-HCl pH 7.5] to 100 μM. Protein concentration was determined by Bradford assay. Cleaved CPD variants were biotinylated *in vitro* with GST-BirA enzyme (*7*) and purified on a Superdex 200 10/30 column (GE Healthcare) equilibrated in 10 mM Tris-HCl, pH 7.4, 150 mM NaCl to remove excess biotin for use in SPR assays.

Purification of CPD for crystallization. For purification of cleaved CPD used for crystallization studies, the affinity purification procedure was performed as described above with the following modifications. His_6-tagged CPD was purified from 3 L culture of BL21(DE3) harboring pET28a-CPDstop, and His_6-tagged CPD was eluted from 1.5 mL NiNTA agarose beads in a final volume of 1 mL elution buffer. The affinity purified His_6-tagged CPD was auto-cleaved by adding 9 mL CPD cleavage buffer containing 100 μM $InsP_6$ and incubating the cleavage reaction at 37ºC for 1 hr. The cleaved CPD was buffer exchanged into lysis buffer using a 10 kDa Centricon concentrator (Millipore), and incubated with 500 μL Ni-NTA agarose beads at 4˚C for 1 hr to pull-down both uncleaved His_6-tagged CPD and the N-terminal His_6-tagged fragment liberated upon auto-cleavage. Binding reactions were pelleted at 1,500 g, and the supernatant containing untagged cleaved CPD was buffer exchanged into gel filtration buffer [250 mM NaCl, 10 mM Tris pH 7.5]. Untagged cleaved CPD (amino acids 3442-3650) was further purified by gel filtration chromatography using an S200 16/60 Sephacryl column (GE Healthcare). The protein was concentrated in gel filtration buffer to a concentration of 30 mg/mL. Protein concentration was determined by measuring the absorbance at 280 nm.

To prepare seleno-methionine (SeMet) substituted cleaved CPD for crystallization studies, an overnight culture of B384(DE3) harboring pET28a-CPDstop was grown in 60 mL minimal media [7.5 mM $(NH_4)_2SO_4$, 30 mM KH_2PO_4, 60 mM K_2HPO_4, 800 mg/L 19 amino acid mix excluding methionine, 5% w/v glucose, 1 mM $MgSO_4$, 4 mg/L thiamine, 4 mg/L D-biotin, 50 mg/L SeMet (Sigma)] supplemented with 5% LB media. The overnight culture was diluted 1:100 in 5 L minimal media and grown for 6 hr until an OD_{600} of 0.6 was reached. Cultures were induced with 350 µM IPTG and grown at 37ºC for an additional 4 hr. SeMet-substituted cleaved CPD was purified using a similar protocol to native cleaved CPD. SeMet substitution at both methionine sites was confirmed by intact mass spectrometry using a Fourier Transform mass spectrometer (LTQ-FTMS, Thermo-Finnegan).

Crystallization and data collection. For crystallization trials, native and seleno-methionine substituted N-terminal cleaved RTX CPD was concentrated to 1 mM (~30 mg/mL) in 10 mM Tris pH 7.5 and 250 mM NaCl. A twofold excess (2 mM) of $InsP_6$ (Calbiochem) was added before crystallization. Small needle-like crystals were initially obtained using the sitting-drop vapor diffusion method from the Synergy 64 crystallization screen (Emerald Biosystems) in 30% PEG 3350, 30% isopropanol, Tris-HCl pH 8.5. We were unable to obtain crystals of the RTX CPD in the absence of $InsP_6$ in any conditions. Diffraction-quality crystals were ultimately grown in an equal volume of 100 mM Tris-HCl pH 8.5, 30% PEG 3350, and 15% MPD at 22ºC. Se-Met crystals were grown by microseeding with native crystals. Crystals were flash frozen in liquid nitrogen using the mother liquor as a cryoprotectant, and data was collected under cryo-cooled conditions at 100 K. A 2.1Å native data set was collected at beamline 11-1 at the Stanford Synchotron Radiation Laboratory and a 2.8Å Se-Met data set was collected at beamline

8.2.1 at the Advanced Light Source (UC-Berkeley). Diffraction data were processed with HKL2000 (*8*). Data processing statistics are listed in Table S1.

Structure determination and refinement. Initial phases were obtained from a seleno-methionine data set collected at the peak absorption wavelength of 0.9798 Å by single wavelength anomalous dispersion (SAD). Eight selenium heavy atom positions were obtained using SHELX (*9*), corresponding to two sites in each of the four molecules in the asymmetric unit. Initial phases were calculated using SHARP (*10*), with anomalous phasing power of 1.428 and a figure-of-merit of 0.351. Solvent-flattened electron density maps generated by SOLOMON (*11*) were of high enough quality to allow for automated model building by ARP/wARP (*12*) of the central beta-sheets, and further building of helices and loop regions into the experimentally phased 2.8Å SAD map was performed with COOT (*13*). This *de novo* protein model went through initial rounds of simulated annealing in CNS (*14*) using the selenium peak wavelength data. This intermediate model was then used to solve a 2.1Å native data set by molecular replacement using PHASER (*15*). The model was refined with CNS against the 2.1Å data set by iterative rounds of simulated annealing, positional minimization, b-factor refinement, and model adjustment. The final model went through restrained refinement with REFMAC (*16*) resulting in final R_{work} and R_{free} values of 19.9% and 24.3%, respectively. Ramachandran analysis by PROCHECK (*17*) indicates 88.5% of residues reside in the most favorable regions, while 11.5% reside in the additionally allowed regions. Refinement statistics can be found in table S1. Hydrogen bond contacts were calculated using Contact from the CCP4 program package (*18*) and buried surface area was calculated using CNS. Structural figures were

prepared using PyMol (*19*), and electrostatic surface potential was calculated with APBS (*20*) contoured at +/-5 kT/e. Structural comparisons were made using the DALI server (*21*).

The final model consists of two RTX CPD molecules in the asymmetric unit, with chain A consisting of amino acids 1-205 and chain B consisting of residues 5-205. Density for residues 1-4 in chain A is seen extending away from the active site to make crystal contacts with another CPD molecule in the lattice, not with its cognate polypeptide chain, hence Ile5 is cited as the first residue in the model. Chain B is used for all figures in the paper. One $InsP_6$ molecule is seen bound to each CPD molecule, and a single Na+ ion is modeled into the structure of each CPD molecule coordinated by the C1 and C2 phosphates and main chain carbonyl of Glu27.

Surface Plasmon Resonance (SPR) Measurements. SPR measurements were performed at 25ºC using a Biacore T100 instrument equilibrated in 10 mM Tris-HCl, 150 mM NaCl, pH 7.4 (TBS). After pretreatment of the streptavidin-coupled (SA) chip, ~4000 RU biotinylated CPD was immobilized on each channel leaving one flow channel as a blank (streptavidin alone) control. The chip was then treated with 1 μM biotin to occupy remaining SA binding sites. Preliminary experiments indicated that catalytically active CPD could cleave itself off the chip while exposed to $InsP_6$, so it was necessary to pre-treat the chip with a TBS solution containing 1 mM $InsP_6$ and 100 μM N-ethylmaleimide to neutralize protease activity. Both iodoacetic acid-neutralized CPD and a catalytic cysteine-to-alanine (C140A) mutant had similar $InsP_6$ binding affinities (Fig. 4 and data not shown), indicating that coupling of a maleimide to the catalytic cysteine did not appreciably affect $InsP_6$ binding. For binding measurements, $InsP_6$ was diluted in TBS and three consecutive dilution series (0.01-125 μM) were flowed over the chip at 50

μL/min (150 μL/180 s injection, 500 s wash). Binding affinities were calculated using the Biacore T100 Evaluation software.

Fluorogenic substrate cleavage assay. 1.1 μM of N-terminally His_6-tagged full-length CPD (corresponding to RTX amino acids 3391-3650) was mixed with 1.1 x the indicated concentration of Z-GGL-AMC (BioMol) in cleavage assay buffer (60 mM NaCl, 20 mM Tris pH 7.5, 250 mM sucrose). 90 μL of the enzyme-substrate mixture was added to flat bottom 96 well plates (black). 10 μL of $InsP_6$ (10-fold stock of the indicated concentration, Calbiochem) was added to the enzyme-substrate mixture to initiate the substrate cleavage reaction. Hydrolysis of Z-GGL-AMC by recombinant CPD was followed using a Molecular Devices fmax plate reader at 37ºC. Cleavage of the substrate as a function of time was followed by monitoring the emission at 460 nm following excitation at 380 nm. The initial velocity was determined from the linear portion of progress curve and plotted against $InsP_6$ concentration (to generate the $InsP_6$ activation curve) and against Z-GGL-AMC concentration (to generate the substrate saturation curve). The Michaelis-Menten function on KaleidaGraph (KaleidaGraph) was used to determine the K_a ($InsP_6$ concentration at which V_o cleavage rate is half-maximal at a given Z-GGL-AMC concentration) and K_m (substrate concentration at which V_o cleavage rate is half-maximal at a given $InsP_6$ concentration). It should be noted that no substrate cleavage was observed in the absence of $InsP_6$, emphasizing the strict dependence for CPD protease activity on $InsP_6$. A high concentration of CPD was used in this assay given that low levels of substrate turnover was observed at lower concentrations of CPD, a finding that likely reflects low catalytic efficiency for the fluorogenic peptide substrate.

Fluorescent labeling of recombinant CPD. Wildtype (wt), R182Q/K183N ($InsP_6$ binding mutant) or C140A (catalytic mutant) CPD at 1 μM in 50 μL cleavage assay buffer was either untreated; treated with 0.5 μL of a 20 mM fluorescein 5-maleimide (FLUOR-5-M, Pierce, stock prepared fresh in PBS) to give a 200 μM final concentration; or 0.5 μL of a 100 x stock of the indicated $InsP_6$ concentration; or simultaneously treated with 1.0 μL of a 10 mM FLUOR-5-M: 50 x stock $InsP_6$ mixture. The reactions were incubated for 30 s at room temperature and FLUOR-5-M labeling was quenched by the addition of 5 μL of a 100 mM N-ethylmaleimide stock (Sigma, prepared fresh in PBS). SDS-PAGE loading buffer was added to reactions, and samples were boiled at 95ºC or 3 min and resolved by SDS-PAGE on a 15% gel. Gels were washed briefly in deionized water, and fluorescent labeling of the active site cysteine was visualized by excitation at 532 nm and emission at 580 nm using a Typhoon scanner (GE Healthcare). Labeling reactions were then visualized by Coomassie stain. No labeling of C140A by FLUOR-5-M was observed, while residual FLUOR-5-M labeling of the catalytic Cys was observed for the R182Q/K183N $InsP_6$ binding mutant irrespective of the presence of $InsP_6$.

Western blot analysis of RTX toxin. For detection of RTX in supernatant fractions, overnight *V. cholerae* strains grown at 37ºC in LB shaking were diluted 1:100 into 3.5 mL LB media. Diluted cultures were grown to mid-log phase (OD_{600} ~0.5, ~2.25 hr growth) then pelleted at 5,000 x g for 5 min. The resulting supernatant was precipitated in 10% tricholoroacetic acid (TCA, final concentration) and incubated for 1 hr on ice. Precipitates were pelleted at 10,000 x g for 10 min, washed once with 1 mL cold acetone, and the resulting pellet was re-suspended in 125 μL of LDS (Invitrogen) loading buffer containing 0.01 N NaOH and 5 mM DTT. Samples were heated to 70ºC for 10 min then loaded onto a 3-8% Tris-Acetate pre-cast gel (Invitrogen).

Following transfer to nitrocellulose, RTX was detected by Western blotting using a polyclonal antibody raised against recombinant His_6-tagged CPD (amino acids 3391-3650, CoCalico Biologicals) at a 1:5000 dilution, an anti-rabbit IgG HRP antibody (BioRad), and the ECL detection method (ECL Plus, GE Healthcare).

Actin crosslinking assay. HFF cells were seeded into 24-well treated plates and grown to 100% confluency (~1 x 10^6 cells), washed once with pre-warmed DMEM, and left in 0.5 mL DMEM per well. 5 μL of *V. cholerae* supernatants harvested as described above were added to HFF cells and incubated for 2.5 hr at 37ºC. For actin crosslinking experiments involving intact *V. cholerae*, 0.5 mL of a log phase culture (1:100 dilution in LB grown for 2.25 hr) was pelleted, washed once with PBS, and re-suspended in an equal volume of PBS. 5 μL of each washed *V. cholerae* culture was added to HFF cells and incubated for 90 min at 37ºC. 100 μL of 2X SDS-PAGE sample buffer was added directly to each well and incubated shaking at room temperature for 5 min. Cell lysates were collected, boiled at 95ºC for 5 min, then resolved on 4-12% Bis-Tris pre-cast gels (Invitrogen) and transferred to nitrocellulose. Actin was visualized using a polyclonal anti-actin antibody at 1:1000 dilution (Sigma), and a 1:5000 dilution of anti-rabbit IgG HRP (Biorad).

Circular dichroism (CD) spectroscopy. CD data were collected on an Aviv 202-01 spectrometer (Aviv Biomedical) in a cell with path length of 1 mm. Recombinant cleaved wildtype RTX CPD (3442-3650) was diluted to 10 μM in 4 mM Tris-HCl pH 7.4 and 100 mM NaCl ± 20 μM $InsP_6$. Protein concentrations were determined by absorbance at 280 nm. Data

were collected at 25º C in 1 nm steps and with a 1 s averaging time from 260 to 195 nm, and each curve is an average of three sequential scans.

Supporting Figures

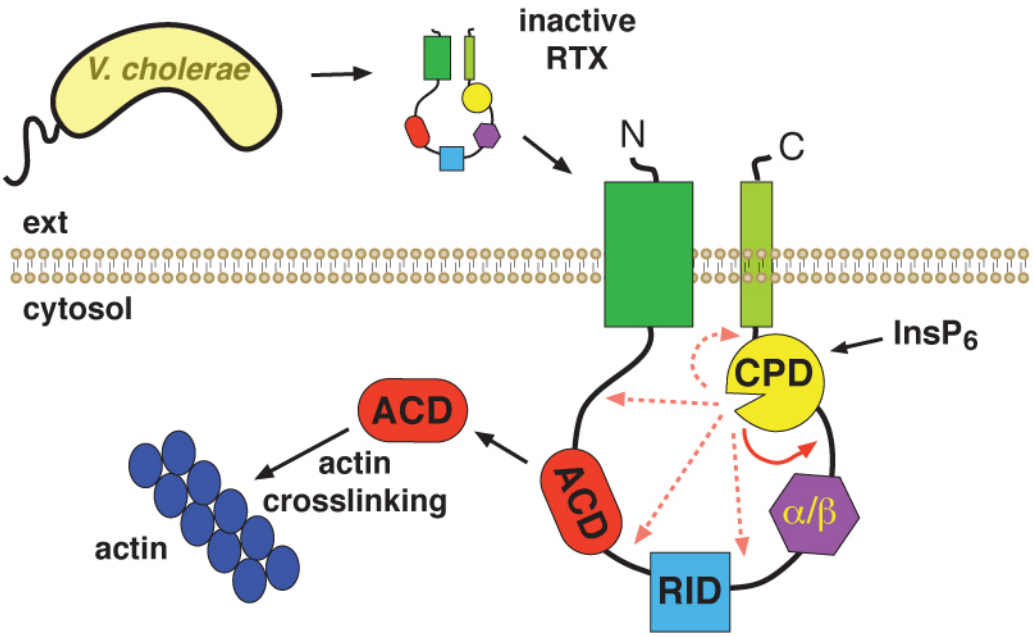

Figure S1. Schematic depicting the proposed model for RTX toxin secretion and entry into the host cell. The inactive pro-toxin is secreted intact into the extracellular environment, in the absence of host cell co-factors. Insertion into the eukaryotic host cell causes activation of the cysteine protease domain (CPD), autocleavage of the polypeptide chain and release of toxin effector domains into the cytoplasm. $InsP_6$, inositol hexakisphosphate; ACD, actin crosslinking domain; RID, Rho-inactivating domain; α/β, α/β hydrolase-like domain; ext, extracellular.

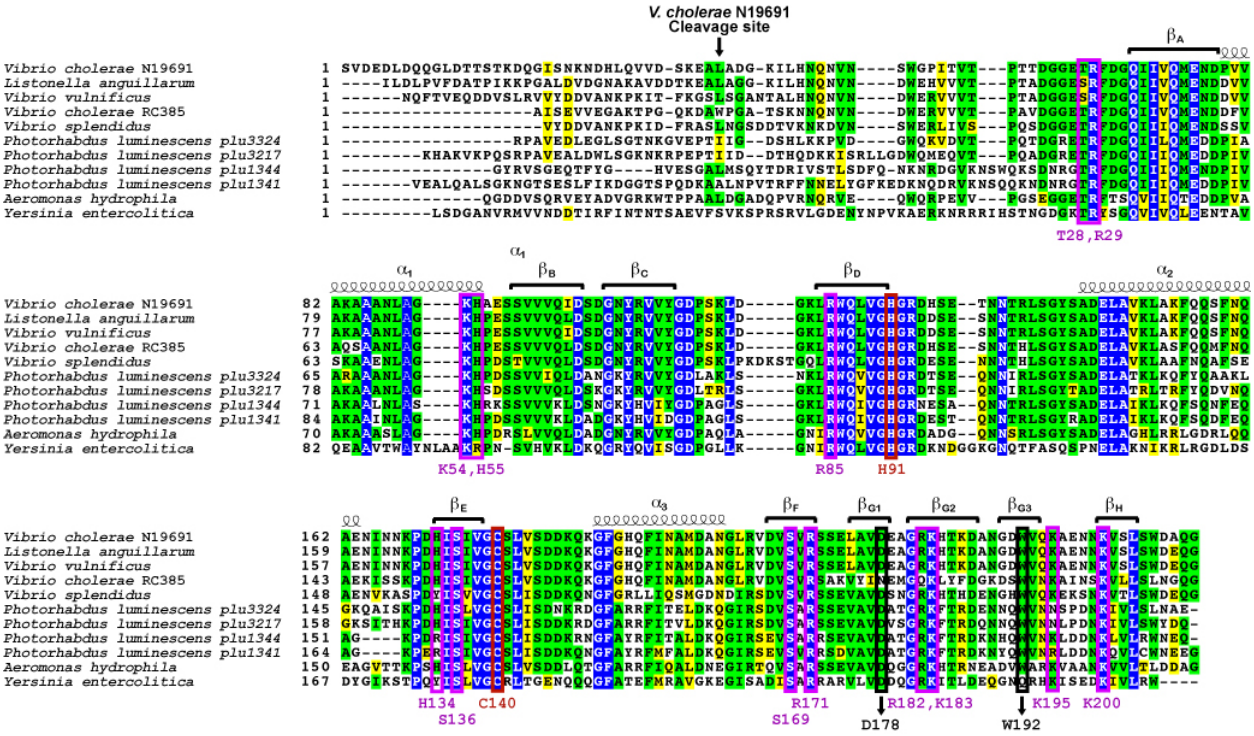

Figure S2. Multiple sequence alignment of the cysteine protease domain from *V. cholerae* N19691 with CPD homologs from related MARTX toxins. Completely conserved identical residues are blocked in blue, conserved identical residues in green, and conserved similar residues in yellow. Secondary structure elements of the *V. cholerae* CPD (residues 3405-3650) are shown above the amino acid sequences and correspond to the labeling in fig. S4D (⟨ denotes ⟨-helix; ® indicates ®-sheet). The catalytic Cys and His residues are boxed and labeled in red. A high degree of conservation is observed among basic cage residues (boxed and labeled in purple) and ®-hairpin residues (boxed and labeled in black), suggesting that the mechanism of $InsP_6$-activation is conserved. The numbering of *V. cholerae* CPD $InsP_6$ binding residues and ®-flap residues is given relative to the core protease domain and starts after the indicated cleavage site for the *V. cholerae* CPD. The sequence alignment was performed using ClustalW; the figure was generated using Boxshade running on the San Diego Supercomputing Server.

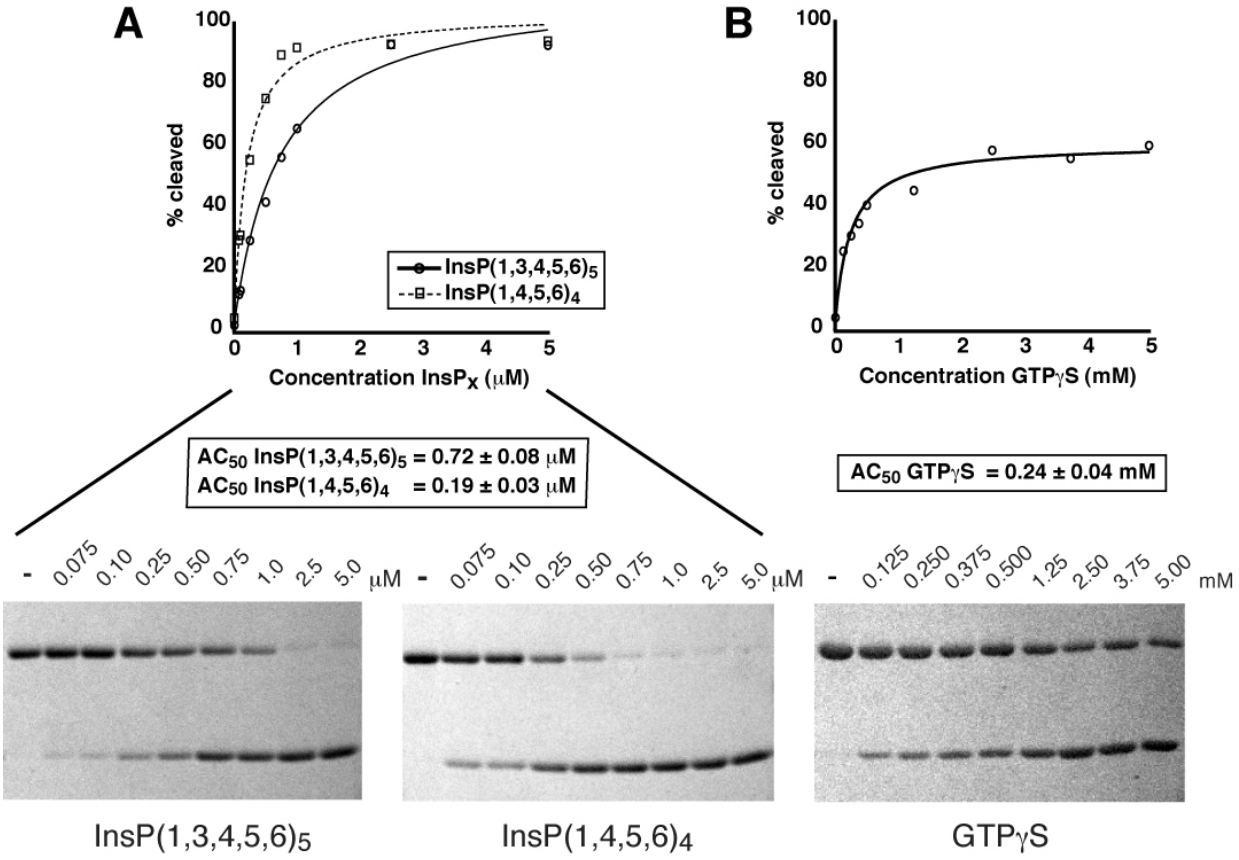

Figure S3. Activation of RTX cysteine protease autocleavage by $InsP_6$ metabolites **(A)** and GTPγS **(B)**. Recombinant RTX CPD (amino acids 3391-3650) was incubated with the indicated concentrations of $InsP(1,3,4,5,6)_5$, $InsP(1,4,5,6)_4$, or GTPγS for 2 h, and autocleavage was assessed by SDS-PAGE and Coomassie staining. The amount of autocleaved CPD versus the total protein amount was analyzed by densitometry and plotted versus concentration of $InsP_6$. Reactions were performed in triplicate and averaged (mean ± SD) before plotting. Gels shown are representative of the three experiments. The concentration of activator required to achieve half-maximal autocleavage is given as the AC_{50}. Autocleavage of RTX CPD was virtually complete when activated with inositol phosphates, while saturating concentrations of GTPγS stimulated only ~60% autocleavage in the same time period, suggesting poor kinetics of GTPγS-

induced autocleavage relative to inositol phosphates.

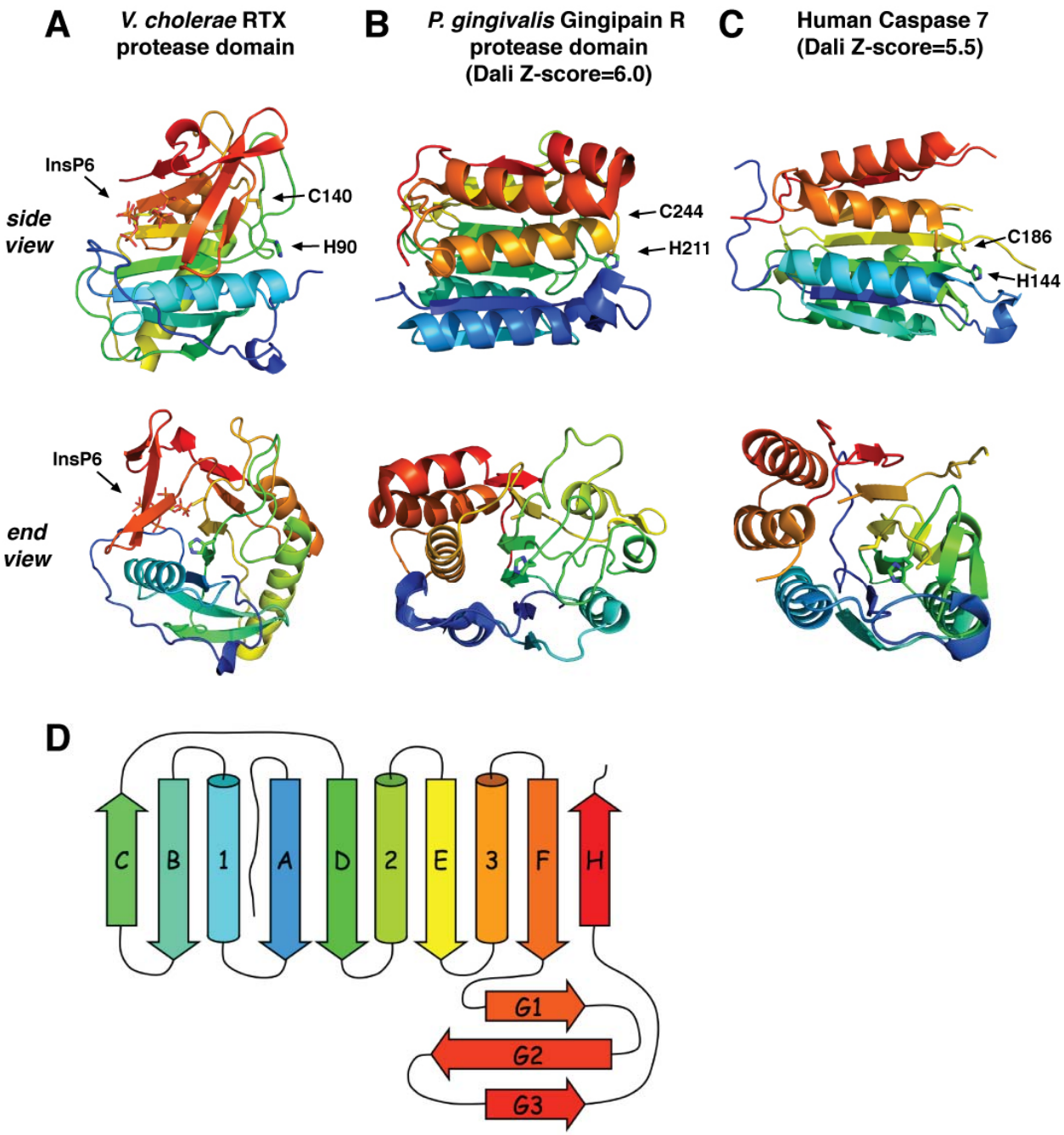

Figure S4. Comparison of the RTX CPD with structurally related proteases. Side and end views of **(A)** the *V. cholerae* RTX cysteine protease domain, **(B)** the Gingipain-R protease domain from *P. gingivalis* (PDB ID: 1CVR), and **(C)** human Caspase-7 (PDB ID: 1SHJ). Proteins are rainbow colored starting with the N-terminus in blue and ending with the C-terminus

in red, and catalytic Cys and His residues are labeled for orientation. Structural alignments were calculated using the DALI server (*21*) (www2.ebi.ac.uk/dali). Gingipain R had a DALI Z-score of 6.0, with an rmsd of 3.8Å and 9% sequence identity (118 out of 432 residues aligned), and Caspase 7 had a DALI Z-score of 5.5, with an rmsd of 4.0Å and 15% sequence identity (111 out of 209 residues aligned). **(D)** Topological diagram of the RTX CPD. Strands are denoted with arrows and helices denoted with cylinders. The rainbow color scheme corresponds to the structure displayed in (A).

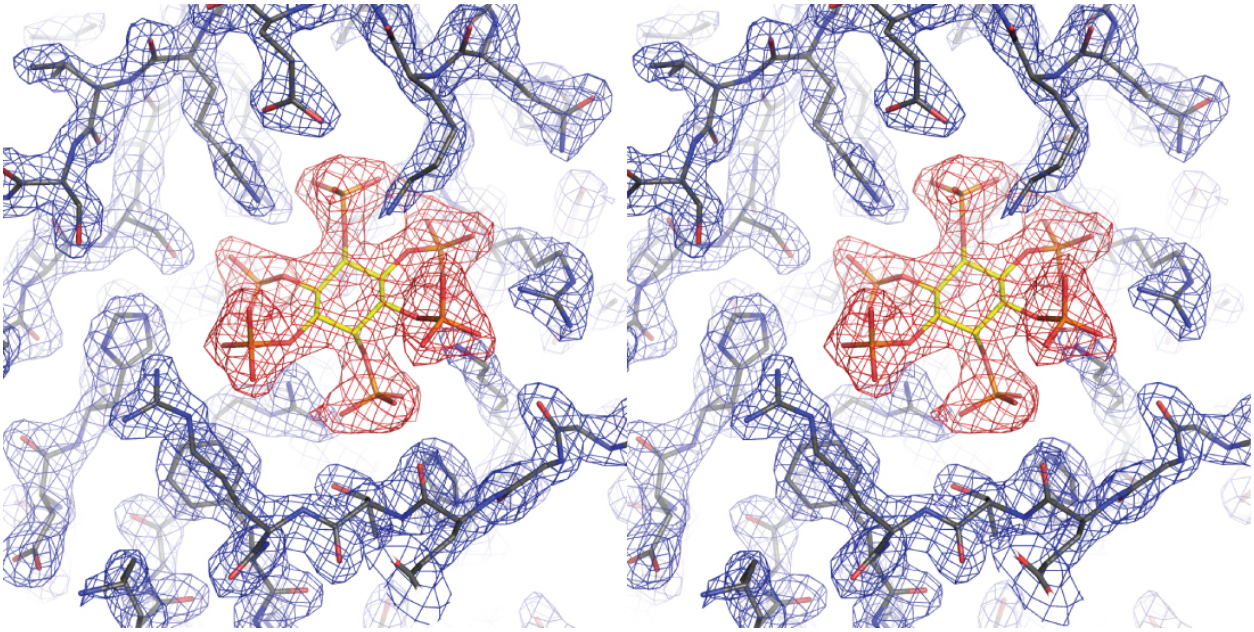

Figure S5. Stereo view of electron density (2Fo-Fc map contoured at 1.5σ) in the $InsP_6$ binding pocket.

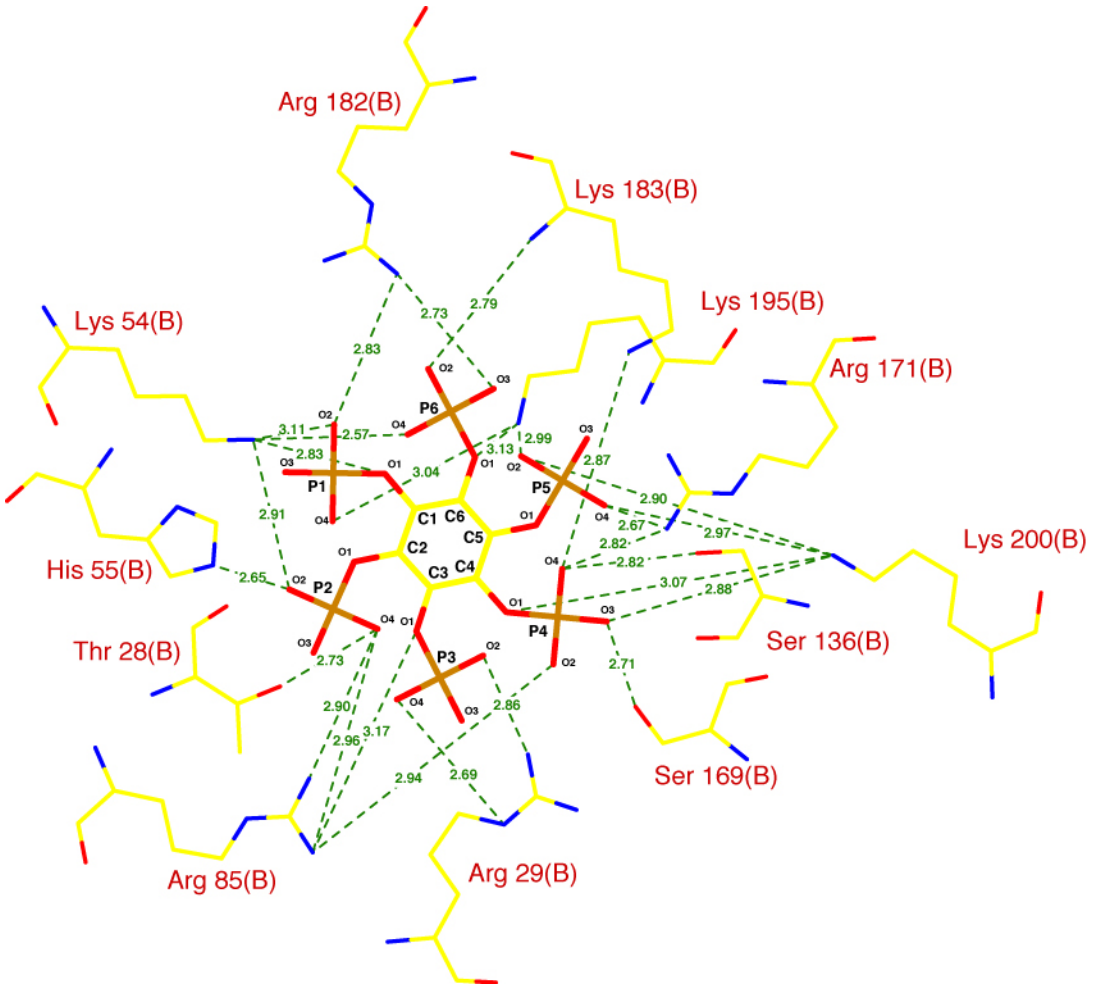

Figure S6. Hydrogen bond interactions between $InsP_6$ and the RTX CPD. The map was generated for CPD chain B using the program LIGPLOT (*22*).

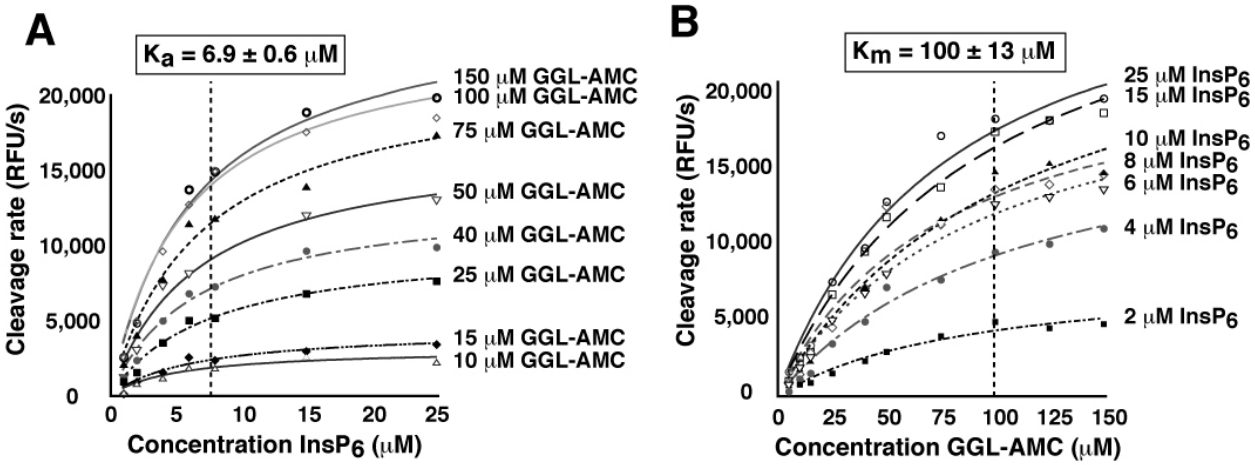

Figure S7. Kinetic analysis of CPD activation by $InsP_6$ suggests an allosteric mechanism of activation. **(A)** $InsP_6$ activation curve for recombinant CPD incubated with varying amounts of GGL-AMC substrate. K_a values for each curve were averaged resulting in a mean of 6.9 ± 0.6 μM (SD). **(B)** GGL-AMC substrate saturation curve for recombinant CPD incubated with varying amounts of $InsP_6$. K_m values for each curve were averaged resulting in a mean of 100 ± 13 μM (SD).

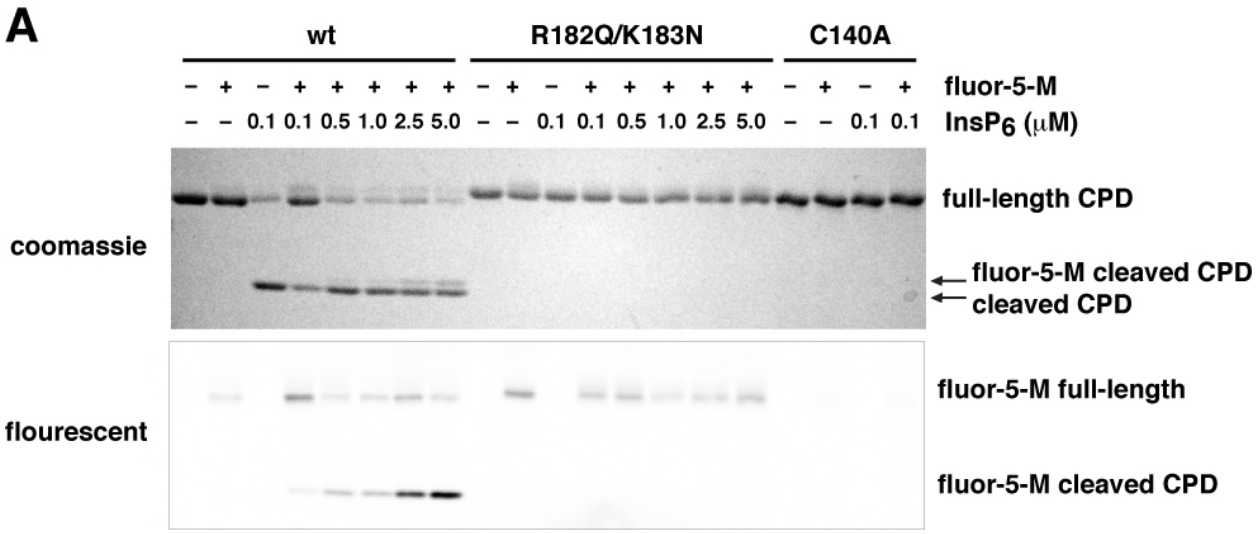

Figure S8. Labeling of recombinant wildtype and mutant CPD active site Cys by fluorescein 5-maleimide (fluor-5-M) in the presence of varying amounts of $InsP_6$. Wildtype (wt), R182Q/K183N ($InsP_6$ binding mutant) or C140A (catalytic-dead) CPD at 1 μM was either untreated, treated with 200 μM fluor-5-M, the indicated concentration of $InsP_6$, or simultaneously treated with fluor-5-M and $InsP_6$. After 30 s, fluor-5-M labeling was quenched by the addition of 10 mM N-ethylmaleimide, and samples were resolved by SDS-PAGE. *Upper panel*, Coomassie stain of labeling reactions, *lower panel*, fluorescent imaging of labeling reactions. The subset of wildtype CPD labeled by fluor-5-M can be observed in the Coomassie stain as a slight decrease in mobility (arrows).

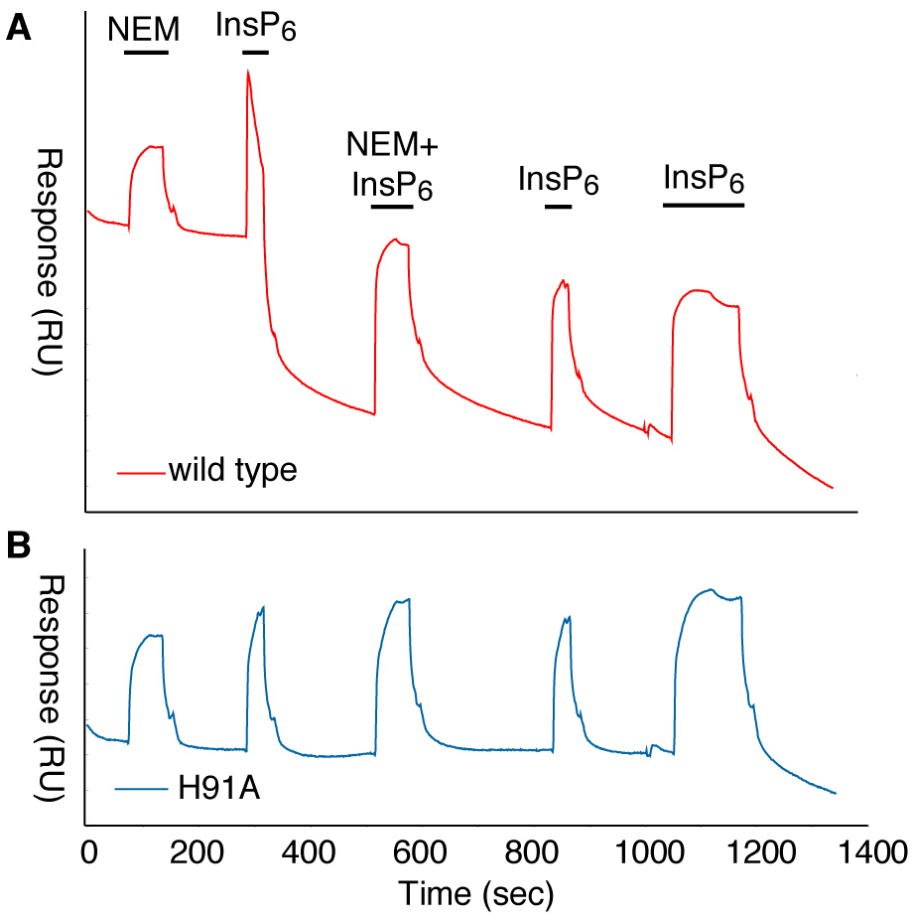

Figure S9. NEM-mediated inhibition of RTX CPD activity in the presence of $InsP_6$. **(A)** Immobilized wildtype or **(B)** catalytically-dead (H91A) CPD was treated with 100 μM N-ethylmaleimide (NEM) for 60 s, followed by 100 μM $InsP_6$ for 30 s. The chip was then treated with 100 μM NEM + 100 μM $InsP_6$ for 60 s, followed by 100 μM $InsP_6$ alone for 30 s and 120 s, respectively. Cleavage of the wildtype but not H91A CPD off the SPR chip upon $InsP_6$ exposure is apparent from the large drop in response units seen in the wildtype channel. No cleavage of wildtype CPD from the chip is seen after treatment of the chip with NEM and $InsP_6$ at the same time. Presumably this cleavage occurs in the biotinylation sequence (LHHILDAQKMVWNHR), which is likely disordered and contains two Leu residues N-terminal to the biotinylated Lys residue.

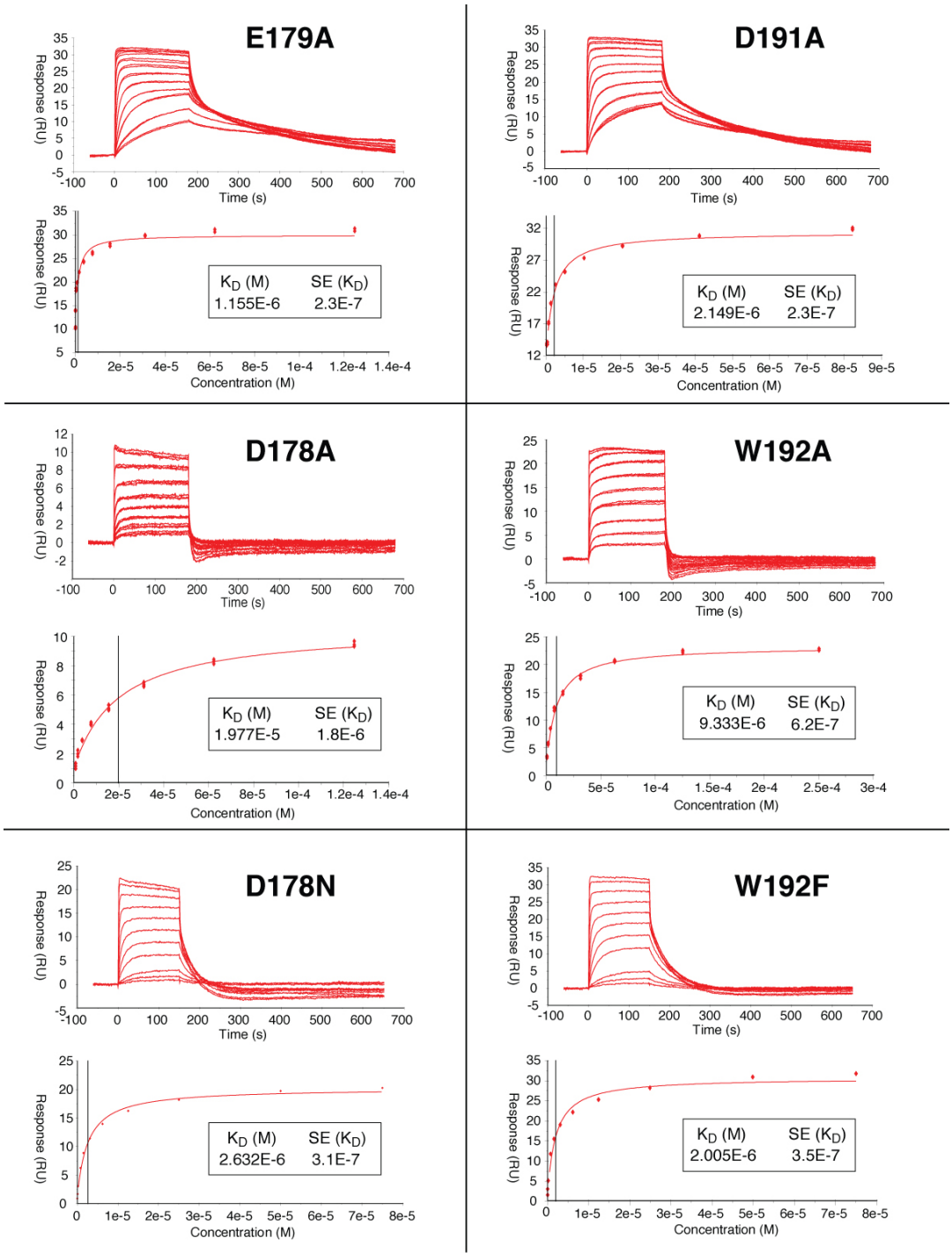

Figure S10. SPR measurements of $InsP_6$ binding to CPD mutants. Sensorgrams and fitted curves are displayed for E179A, D178A, D178N, D191A, W192A and W192N.

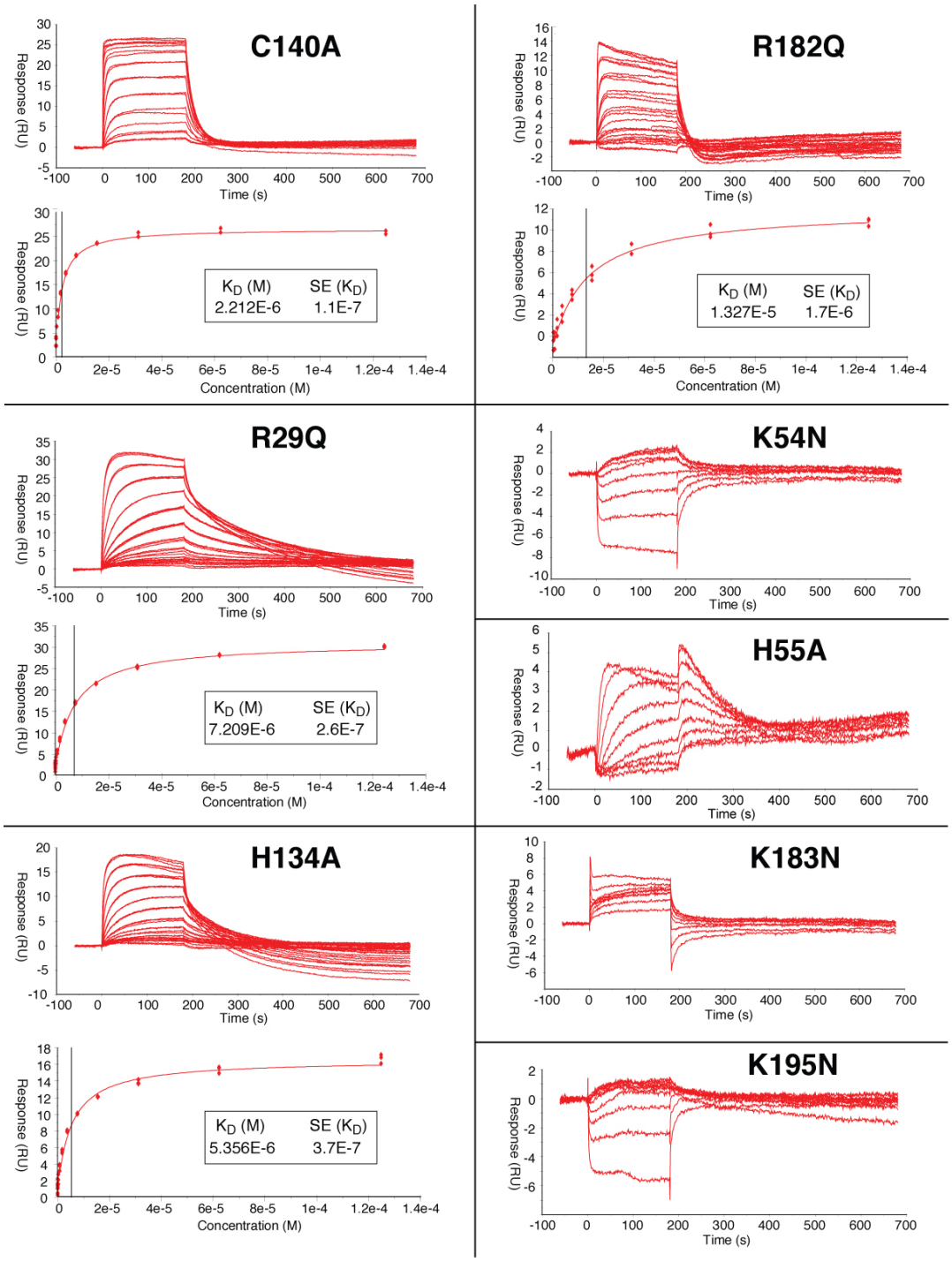

Figure S10. SPR measurements of $InsP_6$ binding to CPD mutants. Sensorgrams and fitted curves are displayed for C140A, R29Q, H134A, and R182Q. For the weakly-binding mutants (K54N, H55A, K195N, and K183N), only the sensorgram is shown due to an inability to obtain a reasonable fit for the data.

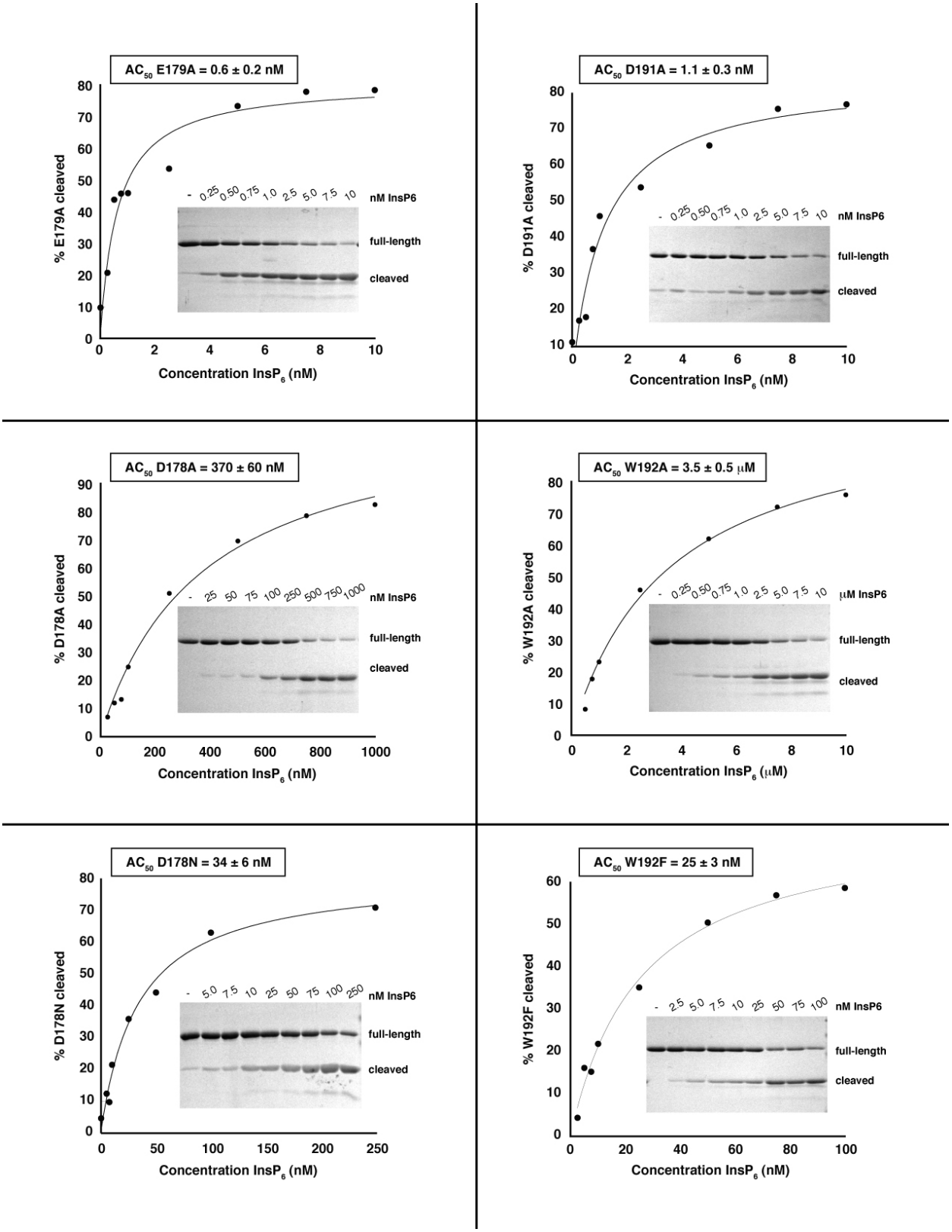
AC50 E179A = 0.6 ± 0.2 nM
% E179A cleaved
Concentration InsP6 (nM)
- 0.25 0.50 0.75 1.0 2.5 5.0 7.5 10
nM InsP6
full-length
cleaved
AC50 D191A = 1.1 ± 0.3 nM
% D191A cleaved
Concentration InsP6 (nM)
- 0.25 0.50 0.75 1.0 2.5 5.0 7.5 10
nM InsP6
full-length
cleaved
AC50 D178A = 370 ± 60 nM
% D178A cleaved
Concentration InsP6 (nM)
- 25 50 75 100 250 500 750 1000
nM InsP6
full-length
cleaved
AC50 W192A = 3.5 ± 0.5 μM
% W192A cleaved
Concentration InsP6 (μM)
- 0.25 0.50 0.75 1.0 2.5 5.0 7.5 10
μM InsP6
full-length
cleaved
AC50 D178N = 34 ± 6 nM
% D178N cleaved
Concentration InsP6 (nM)
- 5.0 7.5 10 25 50 75 100 250
nM InsP6
full-length
cleaved
AC50 W192F = 25 ± 3 nM
% W192F cleaved
Concentration InsP6 (nM)
- 2.5 5.0 7.5 10 25 50 75 100
nM InsP6
full-length
cleaved

Figure S11.

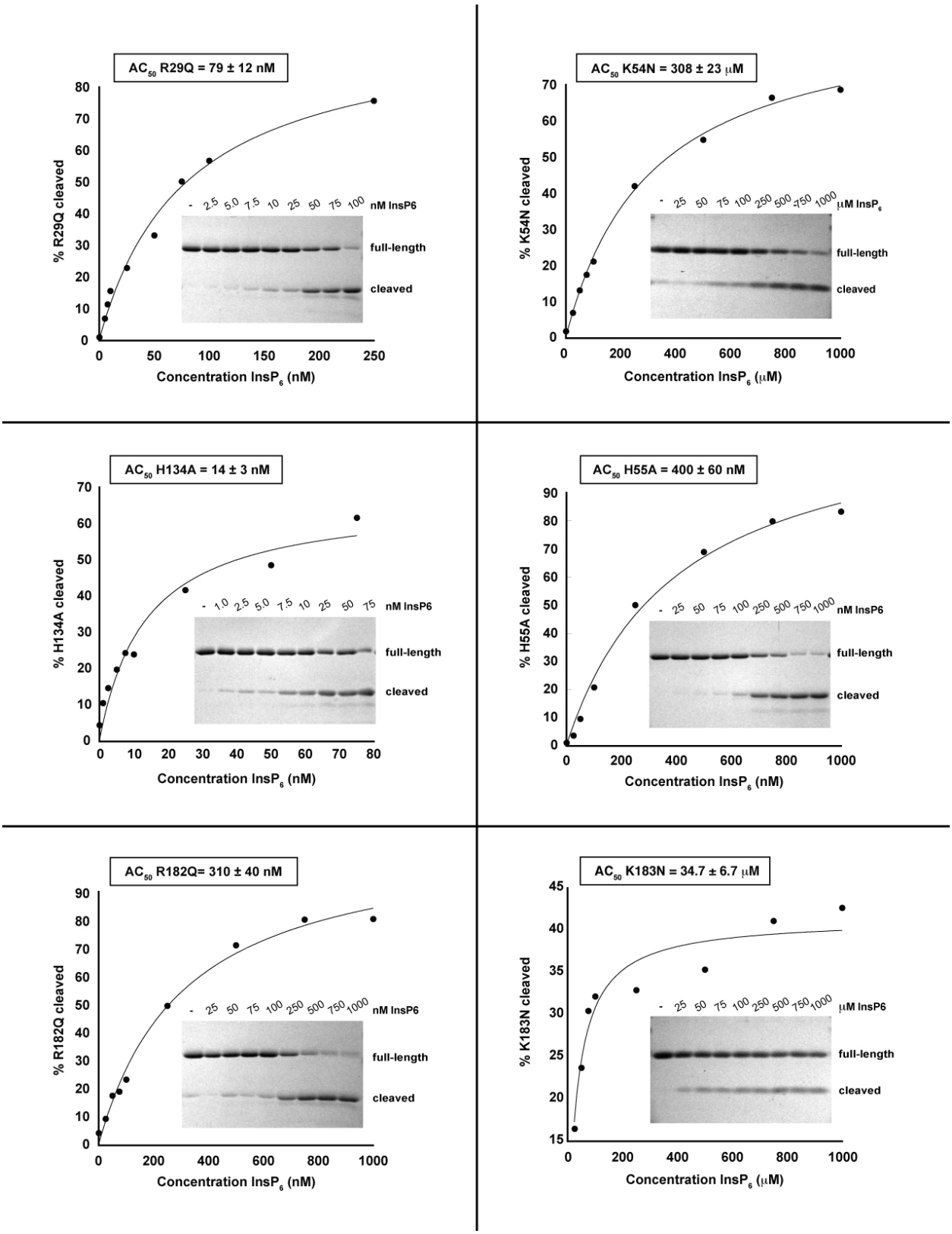
AC50 R29Q = 79 ± 12 nM
% R29Q cleaved
Concentration InsP6 (nM)
- 2.5 5.0 7.5 10 25 50 75 100 nM InsP6
full-length
cleaved
AC50 K54N = 308 ± 23 μM
% K54N cleaved
Concentration InsP6 (μM)
- 25 50 75 100 250 500 750 1000 μM InsP6
full-length
cleaved
AC50 H134A = 14 ± 3 nM
% H134A cleaved
Concentration InsP6 (nM)
- 1.0 2.5 5.0 7.5 10 25 50 75 nM InsP6
full-length
cleaved
AC50 H55A = 400 ± 60 nM
% H55A cleaved
Concentration InsP6 (nM)
- 25 50 75 100 250 500 750 1000 nM InsP6
full-length
cleaved
AC50 R182Q= 310 ± 40 nM
% R182Q cleaved
Concentration InsP6 (nM)
- 25 50 75 100 250 500 750 1000 nM InsP6
full-length
cleaved
AC50 K183N = 34.7 ± 6.7 μM
% K183N cleaved
Concentration InsP6 (μM)
- 25 50 75 100 250 500 750 1000 μM InsP6
full-length
cleaved

Figure S11.

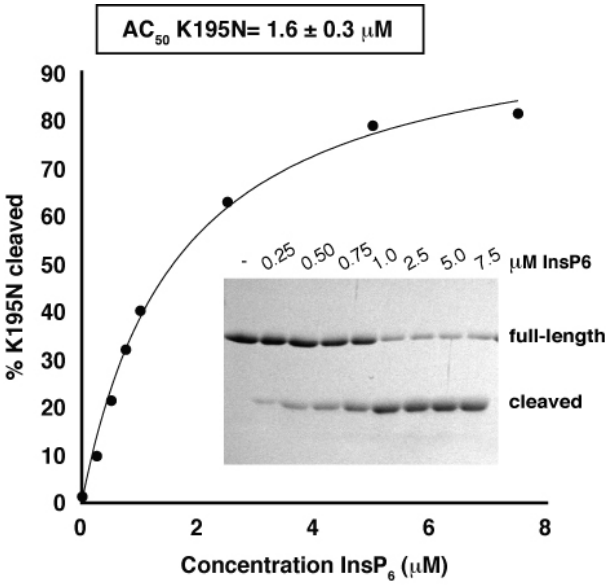

Figure S11. AC_{50} measurements for $InsP_6$-activated autocleavage of CPD mutants. Recombinant RTX CPDs (amino acids 3391-3650) with the indicated mutations were incubated with increasing concentrations of $InsP_6$ for 2 h, and autocleavage was assessed by SDS-PAGE and Coomassie staining (representative gel shown as inset). Reactions were performed in triplicate and the amount of autocleaved protein relative to the total protein amount was analyzed by densitometry, averaged, and plotted versus concentration of $InsP_6$. The AC_{50} was determined as the concentration of $InsP_6$ that produced half-maximal autocleavage. Data are expressed as mean ± SD.

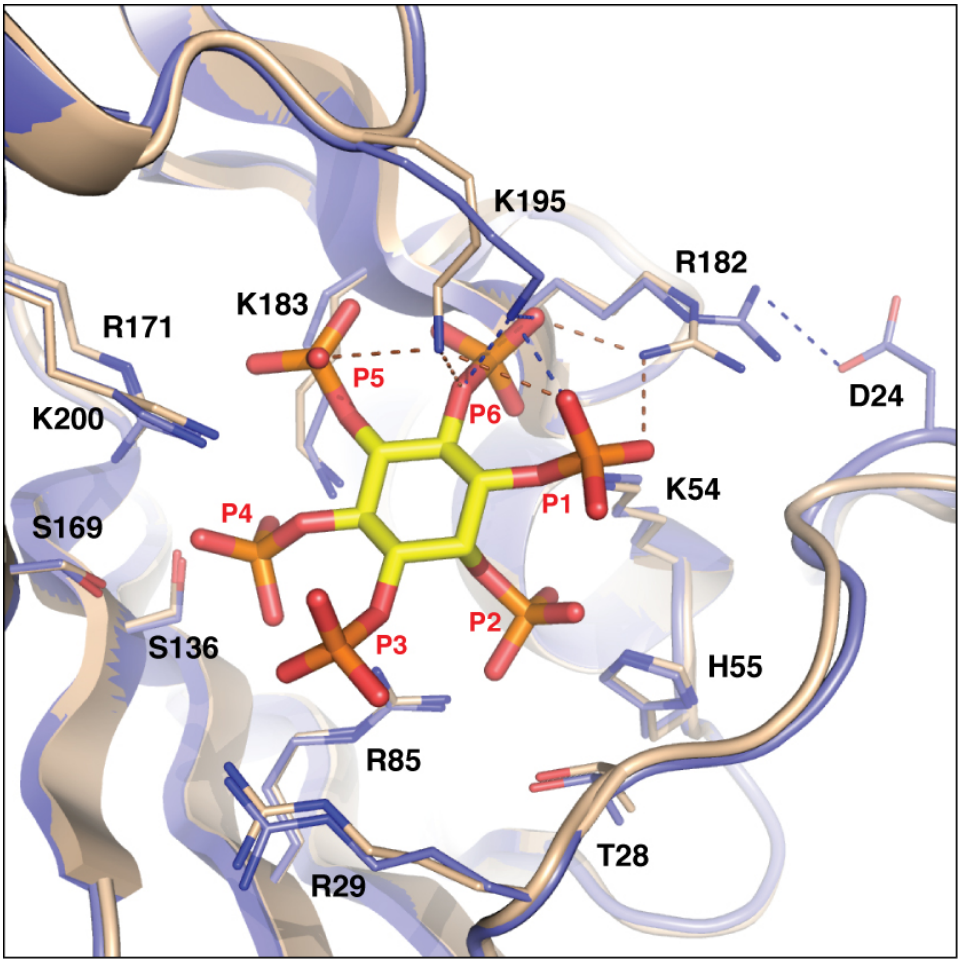

Figure S12. Overlay of $InsP_6$ binding sites for both CPD molecules in the asymmetric unit. Chain A is colored in slate blue, and chain B colored in tan. Nearly all residues involved in $InsP_6$ binding are in the same conformation, except K195 which has two rotamer positions that contact different subsets of oxygens on the $InsP_6$ phosphates, and R182 which also has two rotamer conformations that either contact $InsP_6$ phosphate groups 1 and 6 (chain B) or contact Asp24 and no $InsP_6$ phosphate groups (chain A). Table S2 contains a full list of CPD residue-$InsP_6$ phosphate contacts for each chain.

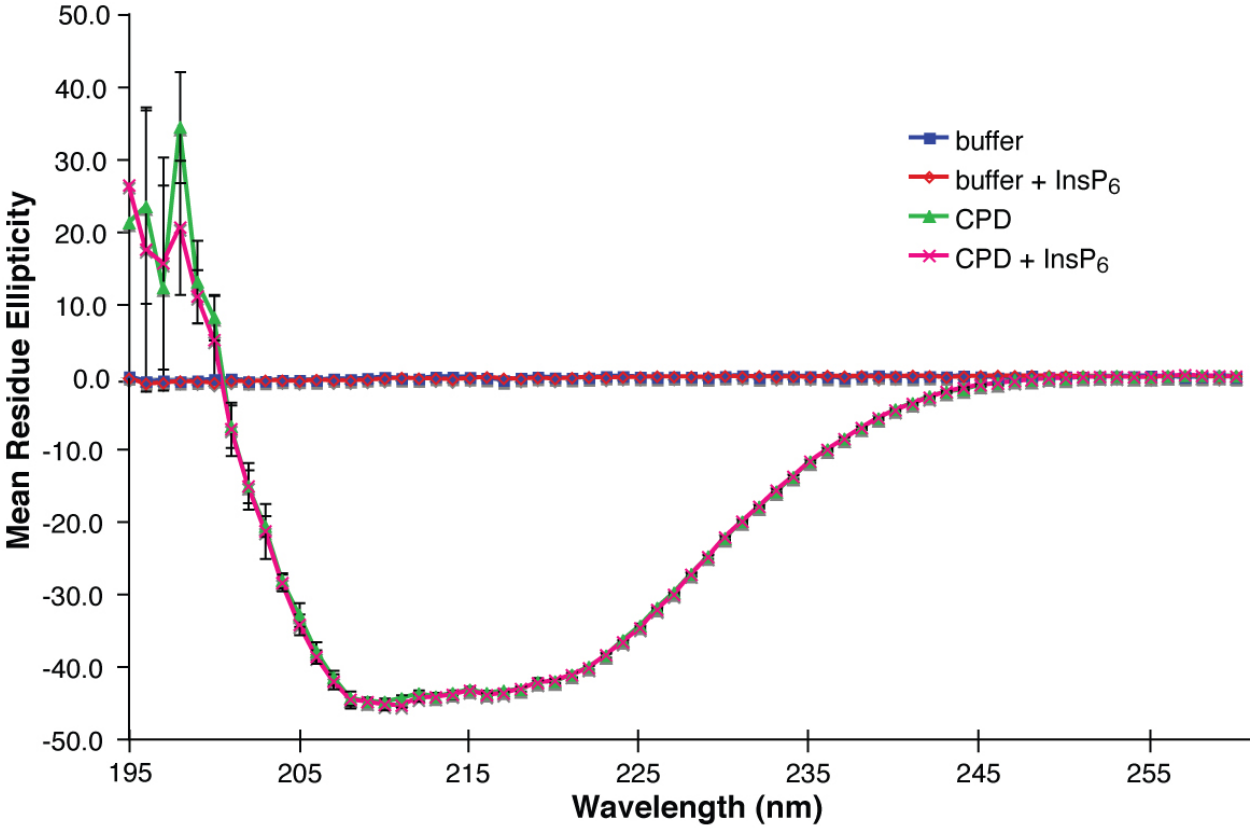

Figure S13. Circular dichroism (CD) spectra of the RTX CPD. Far-UV CD spectra were measured from 260 to 195 nm for buffer, buffer+20 μM $InsP_6$, 10 μM CPD, or 10 μM CPD+20 μM $InsP_6$ and mean residue ellipticity was plotted versus wavelength. Data points represent the mean of measurements ± SD from three consecutive scans.

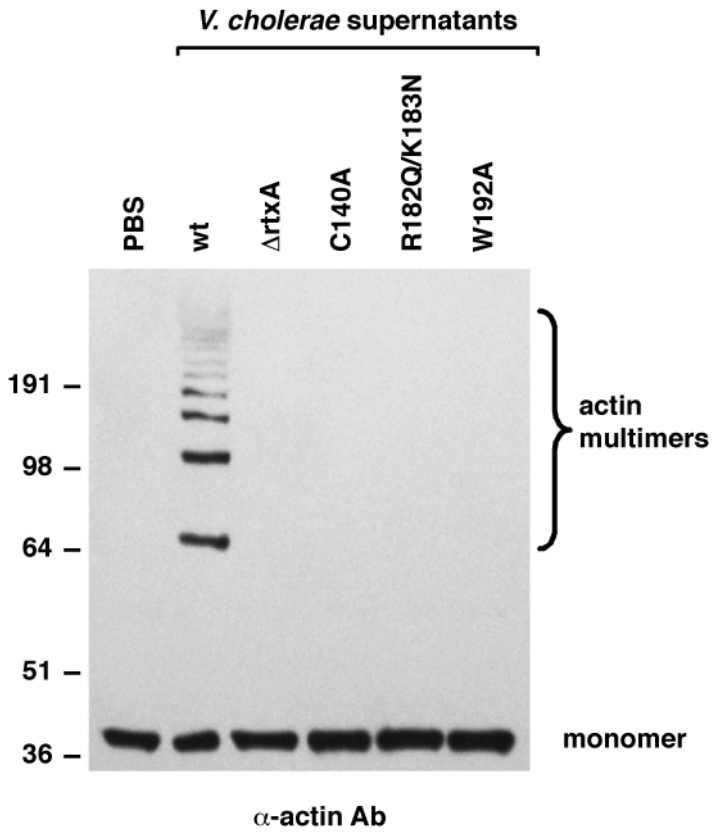

Figure S14. Actin crosslinking induced upon incubation of *V. cholerae* supernatants with HFF cells. Supernatants from *V. cholerae* strains harboring either an intact *rtxA* gene (wt), a null mutation in *rtxA* (Δ*rtxA*), point mutations in the region encoding the CPD domain of RTX (*C140A* is catalytic dead; *R182QK183N* is mutated at two $InsP_6$-binding residues; and *W192A* is a β-flap mutation), or PBS were incubated with HFF cells for 2.5 hr. Cells were then lysed, and actin crosslinking was visualized by Western blotting using an anti-actin antibody. The cross-linked forms of actin are labeled to the right.

Table S1: Data collection, phasing (SAD) and refinement statistics

	Native	SAD
Data collection		
Space group	P212121	P1
Cell dimensions		
a, *b*, *c* (Å)	44.5, 66.1, 136.0	44.7, 64.4, 67.0
α, β, γ (°)	90, 90, 90	88.3, 88.8, 89.6
Wavelength (Å)	1.00	0.9794
Resolution (Å)	30-2.10 (2.18-2.10)	50-2.80 (2.90-2.80)
R_{sym}	0.117 (0.530)	0.053 (0.186)
$I / \sigma I$	15.4 (3.2)	32.7 (5.4)
Completeness (%)	96.3 (97.4)	96.8 (85.0)
Redundancy	6.3 (5.5)	3.8 (3.2)
Refinement		
Resolution (Å)	30-2.10	
No. reflections (total/test)	22101/1178	
R_{work} / R_{free}	19.9/24.3	
No. atoms		
Protein	3118	
Ligand/ion	74	
Water	231	
B-factors		
Protein	28.6	
Ligand/ion	28.1	
Water	32.5	
R.M.S. deviations		
Bond lengths (Å)	0.010	
Bond angles (°)	1.33	

Highest resolution shell in parentheses

Table S2: H-bond contacts between CPD residues and $InsP_6$ phosphates

Residue	CPD Chain A				CPD Chain B		
T28	P2				P2		
R29	P3				P3		
K54	P1	P2	P6		P1	P2	P6
H55	P2				P2		
R85	P2	P3	P4		P2	P3	P4
S136	P4				P4		
S169	P4				P4		
R171	P4	P5			P4	P5	
R182	-				P1	P6	
K183	P4	P6			P4	P6	
K195	P1	P6			P1	P5	P6
K200	P4	P5			P4	P5	
Hydrogen bond cutoff distance=3.4Å							

Table 3: Oligonucleotides used in this study

#	Primer name	Primer sequence (restriction site underlined)	
001	5’ NdeI CPD	GGAATTCCATATGCAATATGCGGATCAAATTGTC	*NdeI*
002	3’ XhoI CPDstop	CCGCTCGAGTTAACCTTGCGCGTCCCAGCTTAG	*XhoI*
003	5’ H134A	ATCAACAACAAACCGGATGCCATCAGTATTGTTGGTTGT	–
004	3’ H134A rev	ACAACCAACAATACTGATGGCATCCGGTTTGTTGTTGAT	–
005	5’ R29Q	ACAGATGGTGGTGAAACCCAGTTCGACGGTCAAATCATC	–
006	3’ R29Q rev	GATGATTTGACCGTCGAACTGGGTTTCACCACCATCTGT	–
007	5’ R182Q	GTAGACGAGGCGGGACAGAAGCATACCAAGGACGCG	–
008	3’ R182Q rev	CGCGTCCTTGGTATGCTTCTGTCCCGCCTCGTCTAC	–
009	5’ H55A	GCCAATTTAGCAGGTAAAGCTGCTGAAAGCAGTGTG	–
010	3’ H55A rev	CACACTGCTTTCAGCAGCTTTACCTGCTAAATTGGC	–
011	5’ K195N	GGCGATTGGGTTCAAAATGCAGAAAACAACAAAGTTTCGCTA	–
012	3’ K195N rev	TAGCGAAACTTTGTTGTTTTCTGCATTTTGAACCCAATCGCC	–
013	5’ K183N	GACGAGGCGGGACGTAATCATACCAAGGACGCGAAT	–
014	3’ K183N rev	ATTCGCGTCCTTGGTATGATTACGTCCCGCCTCGTC	–
015	5’ K54N	GCAGCCAATTTAGCAGGTAATCATGCTGAAAGCAGTGTG	–
016	3’ K54N rev	CACACTGCTTTCAGCATGATTACCTGCTAAATTGGCTGC	–
017	5’ D191A	ACCAAGGACGCGAATGGCGCTTGGGTTCAAAAGGCAGAA	–
018	3’ D191A rev	TTCTGCCTTTTGAACCCAAGCGCCATTCGCGTCCTTGGT	–
019	5’ W192F	AAGGACGCGAATGGCGATTTCGTTCAAAAGGCAGAAAAC	–
020	3’ W192F rev	AAGGACGCGAATGGCGATTTCGTTCAAAAGGCAGAAAAC	–
021	5’ W192A	TTCTGCCTTTTGAACCCAAGCGCCATTCGCGTCCTTGGT	–
022	3’ W192A rev	GTTTTCTGCCTTTTGAACCGCATCGCCATTCGCGTCCTT	–
023	5’ C140A	CACATCAGTATTGTTGGTGCTTCTTTGGTGAGTGACGAC	–
024	3’ C140A rev	GTCGTCACTCACCAAAGAAGCACCAACAATACTGATGTG	–
025	5’ E179A	TCTGAACTGGCCGTAGACGCGGCGGGACGTAAGCATACC	–
026	3’ E179A rev	GGTATGCTTACGTCCCGCCGCGTCTACGGCCAGTTCAGA	–
027	5’ D178N	TCTGAACTGGCCGTAGACGCGGCGGGACGTAAGCATACC	–
028	3’ D178N rev	ATGCTTACGTCCCGCCTCGTTTACGGCCAGTTCAGAACT	–
029	5’ D178A	AGTTCTGAACTGGCCGTAGCTGAGGCGGGACGTAAGCAT	–
030	3’ D178A rev	ATGCTTACGTCCCGCCTCAGCTACGGCCAGTTCAGAACT	–
032	5’ R182QK183N	GTAGACGAGGCGGGACAGAATCATACCAAGGACGCGAAT	–
033	3’ R182QK183N	ATTCGCGTCCTTGGTATGATTCTGTCCCGCCTCGTCTAC	–
034	3’ SalI CPD	ACGCACGTCGACACCTTGCGCGTCCCAGCTTAG	*SalI*
035	5’ NcoI CA	AACCCATGGGCCTCTGGTTACAACGTC	*NcoI*
036	3’ XbaI CA	GACTCTAGAAACACTGTGTTTGCTTTCACC	*XbaI*
037	5’ NcoI Δ*rtxA*	AACCCATGGGTTCATATGCCTGCATCCGGT	*NcoI*
038	3’ XbaI Δ*rtxA*	GACTCTAGACTAACAAAATCTAGTAGAGCT	*XbaI*
039	5’ Δ*rtxA*	CCTAAAAGAAGAGTTTGGCTTTCAGACGTGGTTCACAAAAAA	–
040	3’ Δ*rtxA* rev	TTTTTTGTGAACCACGTCTGAAAGCCAAACTCTTCTTTTAGG	–
041	5’ BirA	P-TCGACCTGCATCATATTCTCGACGCACAGAAAATGGTGTGGAATCATCGTC	
042	3’ BirA	P-TCGAGACGATGATTCCACACCATTTTCTGTGCGTCGAGAATATGATGCAGG	
043	5’ H91A	TGGCAGTTGGTGGGGGCTGGTCGCGACCACTCA	–
044	3’ H91A	TGAGTGGTCGCGACCAGCCCCCACCAACTGCCA	–

Supporting References

1. R. M. Horton, H. D. Hunt, S. N. Ho, J. K. Pullen, L. R. Pease, *Gene* **77**, 61 (1989).
2. K. J. Fullner, J. J. Mekalanos, *Infect. Immun.* **67**, 1393 (1999).
3. A. T. Nielsen *et al.*, *PLoS Pathogens* **2**, 109 (2006).
4. B. K. Boardman, B. M. Meehan, K. J. Fullner Satchell, *J. Bacteriol.* **189**, 1827 (2007).
5. K. L. Sheahan, C. L. Cordero, K. J. Satchell, *EMBO J.* **26**, 2552 (2007).
6. K. J. Fullner, J. J. Mekalanos, *EMBO J.* **19**, 5315 (2000).
7. C. A. O'Callaghan *et al.*, *Anal. Biochem.* **266**, 9 (1999).
8. Z. Otwinowski, W. Minor, *Methods Enzymol.* **276**, 307 (1997).
9. G. Sheldrick, T. Schneider, *Methods Enzymol.* **277**, 319 (1997).
10. E. de la Fortelle, G. Bricogne, *Methods Enzymol.* **276**, 472 (1997).
11. J. P. Abrahams, A. G. Leslie, *Acta Crystallogr.* **D52**, 30 (1996).
12. A. Perrakis, R. Morris, V. S. Lamzin, *Nature Struct. Biol.* **6**, 458 (1999).
13. P. Emsley, K. Cowtan, *Acta Crystallogr.* **D60**, 2126 (2004).
14. A. T. Brunger *et al.*, *Acta Crystallogr.* **D54**, 905 (1998).
15. A. J. McCoy *et al.*, *J. Appl. Crystallogr.* **40**, 658 (2007).
16. G. N. Murshudov, A. A. Vagin, E. J. Dodson, *Acta Crystallogr.* **D53**, 240 (1997).
17. R. A. Laskowski, MacArthur M.W., Moss D.S., Thornton J.M., *J Appl. Crystallogr.* **26**, 283 (1993).
18. E. Potterton, P. Briggs, M. Turkenburg, E. Dodson, *Acta Crystallogr.* **D59**, 1131 (2003).
19. W. L. DeLano, *DeLano Scientific, San Carlos, CA, USA* (2002).
20. N. A. Baker, D. Sept, S. Joseph, M. J. Holst, J. A. McCammon, *Proc. Nat. Acad. Sci. U.S.A.* **98**, 10037 (2001).
21. L. Holm, C. Sander, *Science* **273**, 595 (1996).
22. A. C. Wallace, R. A. Laskowski, J. M. Thornton, *Protein Eng.* **8**, 127 (1995).